

SUPPORTING INFORMATION

Understanding the structure directing action of copper-polyamine complexes in the direct synthesis of Cu-SAPO-34 and Cu-SAPO-18 catalysts for the selective catalytic reduction of NO with NH₃

Alessandro Turrina,¹ Eike C. V. Eschenroeder,¹ Bela E. Bode,¹ Jillian E. Collier,² David C. Apperley,³ Paul A. Cox,⁴ John L. Casci,⁵ Paul A. Wright^{1*}

¹ *EaStCHEM School of Chemistry and Centre of Magnetic Resonance, University of St Andrews, Purdie Building, North Haugh, St Andrews, KY169ST, United Kingdom.*

² *Johnson Matthey Technology Centre, Reading, RG4 9NH, United Kingdom.*

³ *Department of Chemistry, Durham University, South Road, Durham DH1 3LE, United Kingdom.*

⁴ *School of Pharmaceutics and Biomedical Sciences, University of Portsmouth, St. Michael's Building, White Swan Road, Portsmouth, PO1 2DT, United Kingdom.*

⁵ *Johnson Matthey, Chilton PO Box 1, Belasis Avenue, Billingham, TS23 1LB, United Kingdom.*

Content

Figures:

- S1.** PXRD patterns of SAPO-34 synthesised using TEAOH and copper acetate without any polyamines.
- S2.** PXRD patterns of Cu-SAPO-18 synthesised without TEAOH and STA-7 seeds.
- S3.** PXRD patterns of Cu and Ni SAPO-18 synthesised using different starting gel composition.
- S4.** Isotherms for the adsorption of N₂ at 77 K on copper and nickel SAPO-34 and SAPO-18.
- S5.** ²⁹Si, ³¹P, ²⁷Al solid-state MAS NMR spectra for dehydrated as-prepared and calcined Ni-SAPO-34 Ni-SAPO-18.
- S6.** Rietveld plots for calcined, dehydrated Ni-SAPO-34 and Ni-SAPO-18.
- S7.** Structures of calcined Ni-SAPO-34 and Ni-SAPO-18 showing all symmetry related positions of Ni²⁺ cations.
- S8.** PXRD patterns of fresh and hydrothermally treated (900 °C for 1 h) Cu-SAPO-34, Cu-SAPO-18, and Cu-SAPO STA-7.

Tables:

- S1.** Typical wavelengths in nm for UV-visible maxima for Cu and Ni complexes with amino and aza chelating agents.
- S2.** EPR fitted parameters for Cu-TETA and Cu-232 complexes contained within SAPO-34 and SAPO-18 respectively.
- S3.** EPR fitted parameters for the calcined and hydrate Cu-SAPO-34 and Cu-SAPO-18.
- S4.** Atomic coordinates and thermal parameters for calcined and dehydrated Cu-SAPO-34.
- S5.** Selected bond lengths and angles for calcined and dehydrated Cu-SAPO-34.
- S6.** Atomic coordinates and thermal parameters for calcined and dehydrated Cu-SAPO-18.
- S7.** Selected bond lengths and angles for calcined and dehydrated Cu-SAPO-18.
- S8.** Crystallographic data for calcined and dehydrated Ni-SAPO-34 and Ni-SAPO-18.
- S9.** Atomic coordinates and thermal parameters for calcined and dehydrated Ni-SAPO-34.
- S10.** Selected bond lengths and angles for calcined and dehydrated Ni-SAPO-34.
- S11.** Atomic coordinates and thermal parameters for calcined and dehydrated Ni-SAPO-18.
- S12.** Selected bond lengths and angles for calcined and dehydrated Ni-SAPO-18.

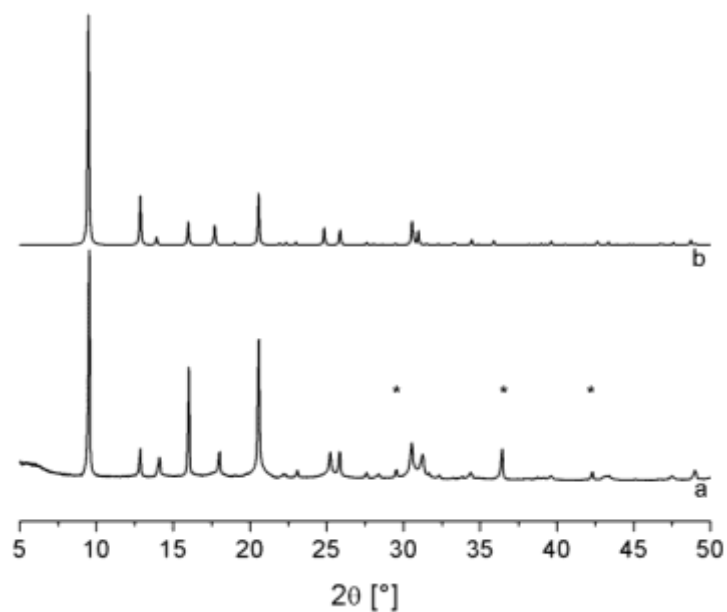


Figure S1. PXRD patterns of SAPO-34 synthesised using TEAOH and copper acetate without any polyamines (a). Simulated pattern of SAPO-34 has been plotted as comparison (b). The peaks marked with an * belong to copper oxide.^{S1}

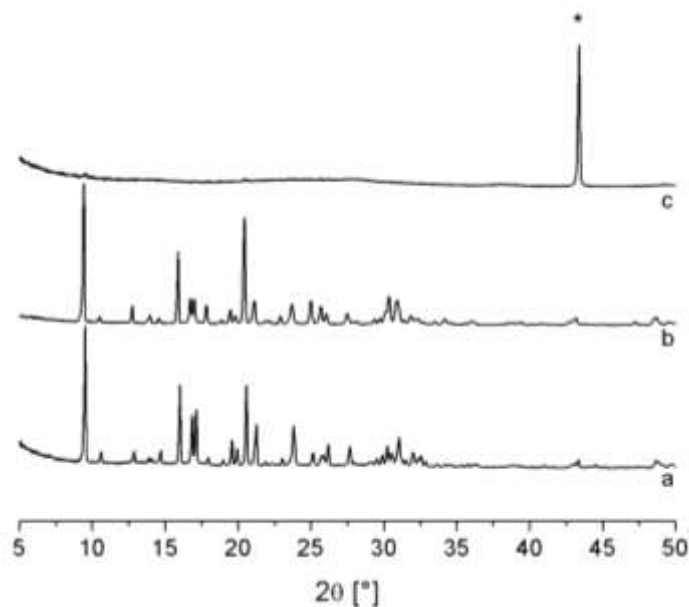


Figure S2. PXRD patterns of the respective synthesis of Cu-SAPO-18 performed using TEAOH as co-base/co-template agent and adding STA-7 seeds (a), without seeds (b) and without TEAOH (replaced by 232) in presence of STA-7 seeds (c). The peak marked with an * belong to the sample holder.

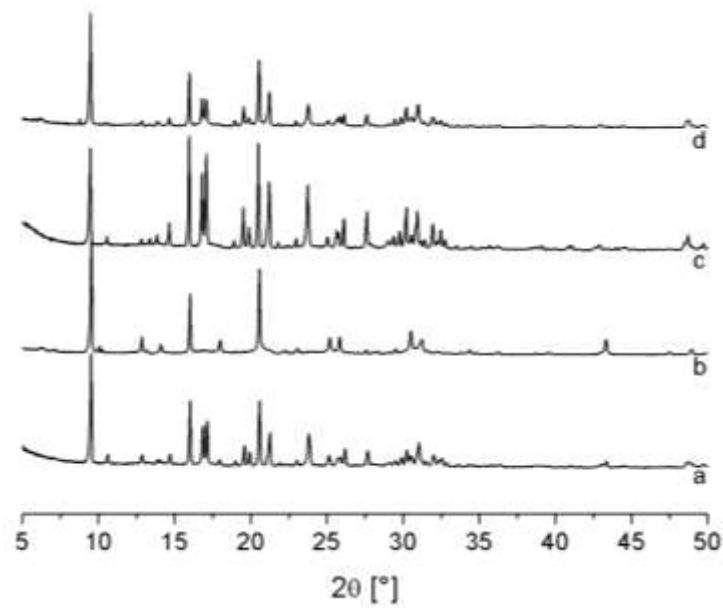


Figure S3. PXRD patterns of Cu and Ni SAPO-18 synthesised using as starting gel $\text{Al}(\text{OH})_3 : 0.61 \text{H}_3\text{PO}_4 : 0.2 \text{SiO}_2 : 40 \text{H}_2\text{O} : 0.06 \text{Cu}^{2+}$ (0.1Ni^{2+}) : 0.2 '232' (a for copper, c for nickel) and $\text{Al}(\text{OH})_3 : 0.8 \text{H}_3\text{PO}_4 : 0.2 \text{SiO}_2 : 40 \text{H}_2\text{O} : 0.1 \text{M}^{2+}$ -232 (b for copper, d for nickel). TEAOH and STA-7 seeds were used with copper as reported in the experimental section.

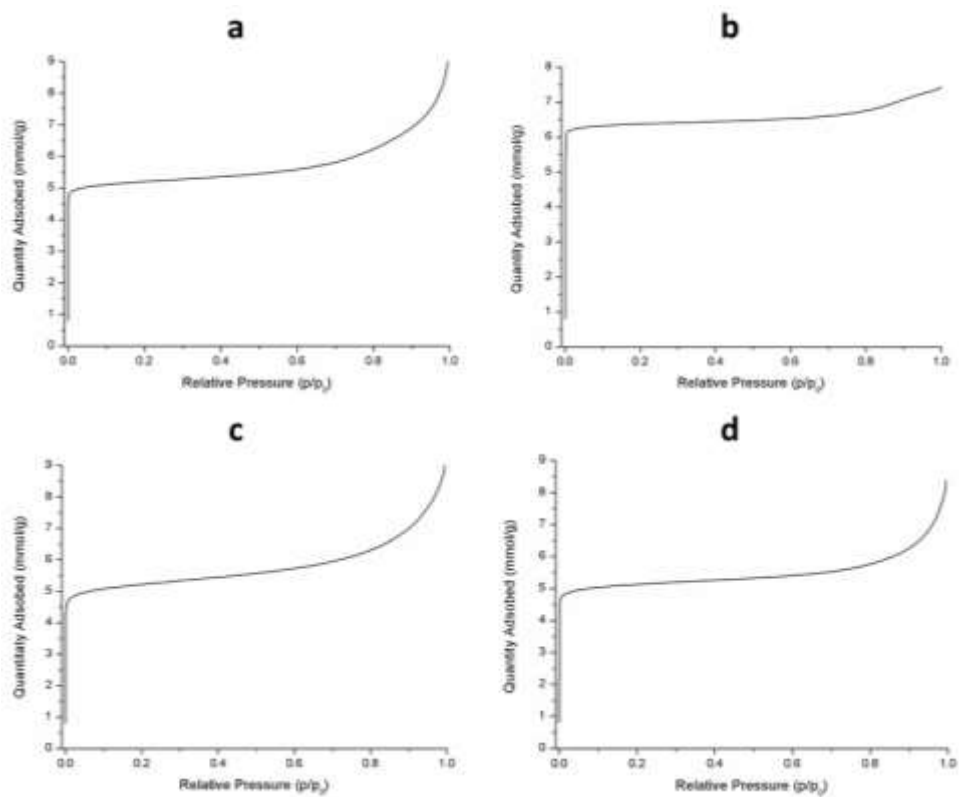


Figure S4. Isotherms for the adsorption of N_2 at $-196 \text{ }^\circ\text{C}$ on calcined Cu-SAPO-34 (a), Ni-SAPO-34 (b), Cu-SAPO-18 (c), Ni-SAPO-18 (d) showing uptakes of 5.2, 6.3, 5.1 and 5.0 mmol g^{-1} at $P/P_0 = 0.2$, respectively.

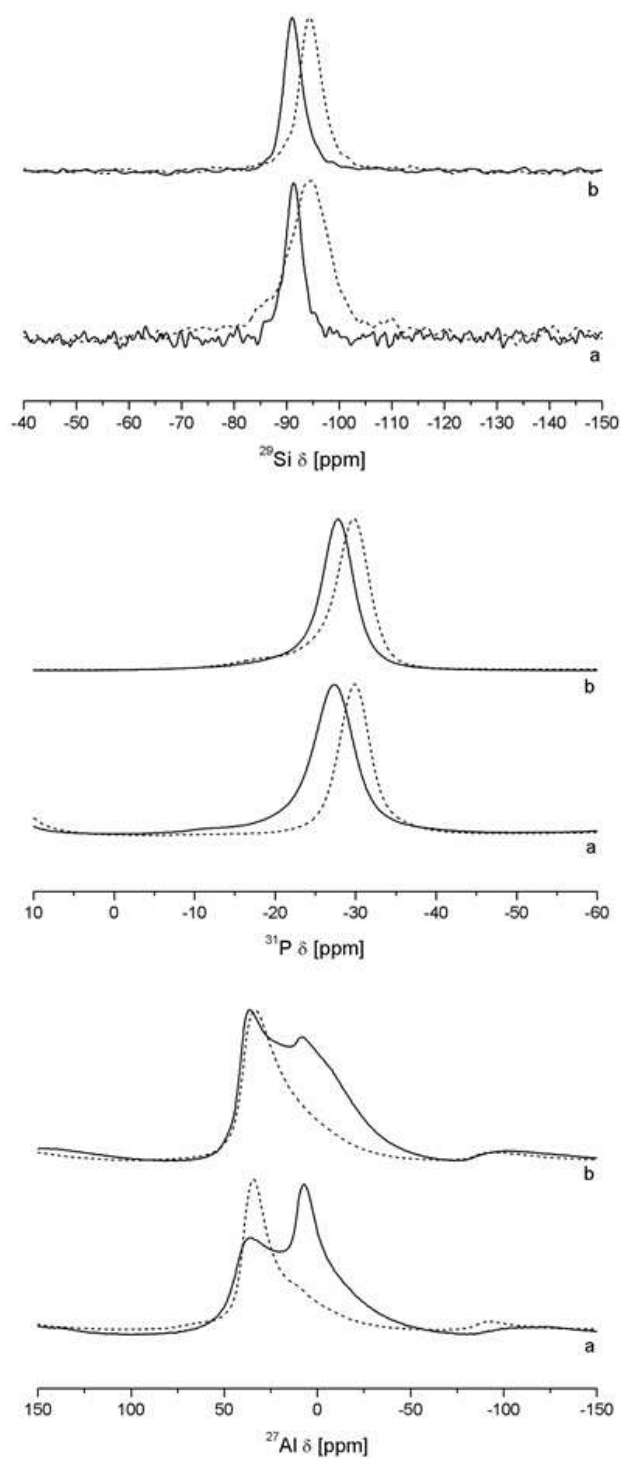


Figure S5. Solid-state MAS NMR spectra for dehydrated as-prepared (solid line) and calcined (dashed line) Ni-SAPO-34 (a) and Ni-SAPO-18 (b). ^{29}Si , (middle) ^{31}P and (bottom) ^{27}Al .

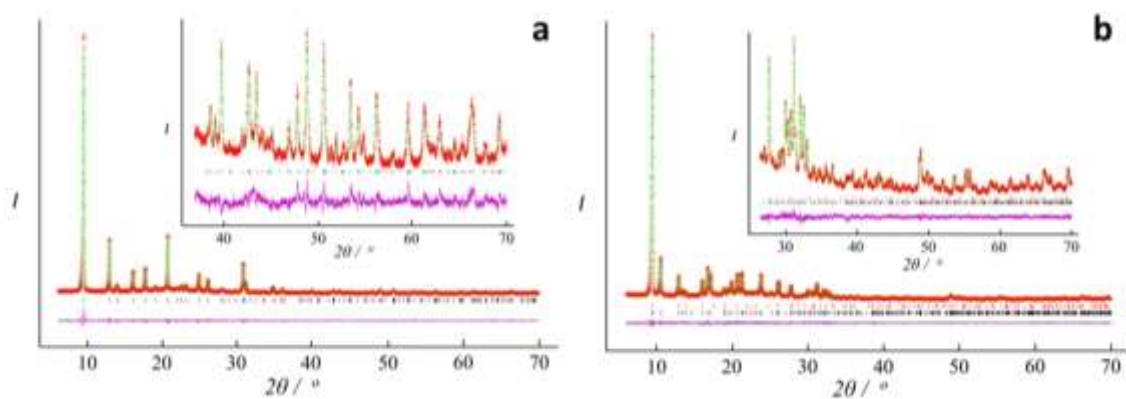


Figure S6. Rietveld plots for calcined, dehydrated Ni-SAPO-34 (a) and Ni-SAPO-18 (b). Observed data (red crosses), calculated fit (green line), and difference plot (purple line). Peak positions are marked in black in (a) while in (b) SAPO-18 peak markers are marked in black and SAPO-34 in red.

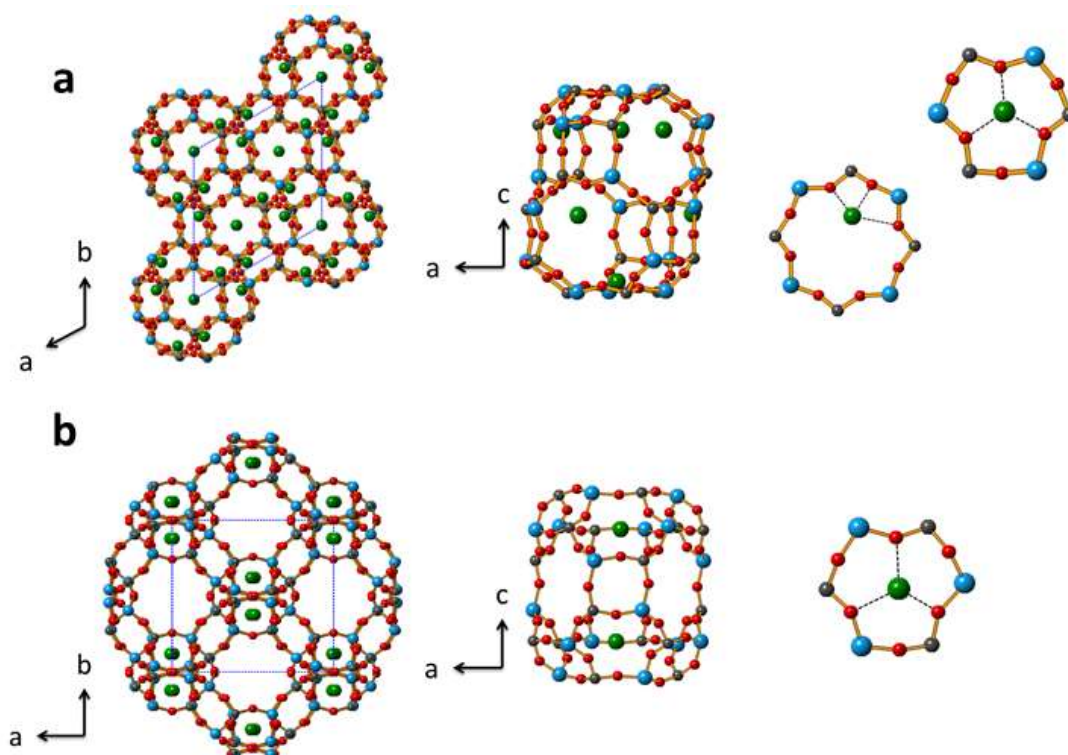


Figure S7. Structures of calcined Ni-SAPO-34 (a) and Ni-SAPO-18 (b) viewed down the c -axis showing all symmetry related positions of Ni^{2+} cations and down the b -axis showing the local environments of Ni^{2+} site. Note that only a small fraction of these sites is occupied. (Al light blue, P dark gray, O red, Ni green).

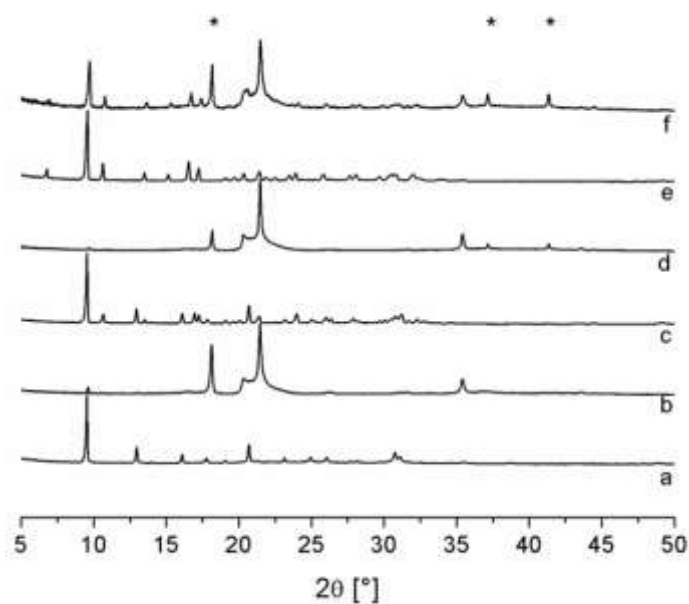


Figure S8. PXRD patterns of fresh and hydrothermally treated (900 °C for 1 h) Cu-SAPO-34, (a and b), Cu-SAPO-18, (c and d), Cu-SAPO STA-7, (e and f). The peaks marked by an asterisk belong to the Teflon disk used during the measurements.

Table S1. Typical wavelengths in nm for UV-visible maxima for Cu and Ni complexes with amino and aza chelating agents.

metal complex	coordination geometry	λ_{max} (nm)
$[\text{Cu}-(\text{DETA})_2]^{2+\text{a}}$	octahedral	630 ^{S2}
$[\text{Cu}-(\text{TETA})]^{2+\text{a}}$	distorted square planar	587 ^{S2}
$[\text{Cu}-(\text{EN})_2]^{2+\text{a}}$	square planar	547 ^{S2}
$[\text{Cu}-(\text{TEPA})]^{2+\text{a}}$	square pyramidal	645 ^{S2}
$[\text{Ni}-(\text{DETA})_2]^{2+\text{b}}$	octahedral	350, 543, 871 ^{S3}
$[\text{Ni}-(\text{cyclam})]^{2+\text{c}}$	square planar	454 ^{S4}

Visible absorption spectra collected at 25 °C in H₂O (a) and CH₃CN (c).

Diffuse reflectance UV–visible spectra of as-prepared $[\text{Ni}(\text{DETA})_2]^{2+}$ -UT-6 (b).

Table S2. EPR fitted parameters for Cu-TETA and Cu-232 complexes contained within SAPO-34 and SAPO-18 respectively.

sample	species weight (%)	g_{\parallel}	g_{\perp}	A_{\parallel} (MHz)	A_{\perp} (MHz)	lw (MHz)
Cu-TETA hydrated	50	2.204	2.067	408	72	450
	50	2.194	2.040	529	60	195
Cu-232 hydrated	75	2.198	2.044	410	40	440
	25	2.189	2.038	564	79	185
Cu-TETA dehydrated	60	2.225	2.052	359	79	390
	40	2.204	2.044	529	60	170
Cu-232 dehydrated	50	2.206	2.059	351	50	420
	50	2.174	2.026	570	42	280
Cu-TETA rehydrated	50	2.204	2.067	408	72	450
	50	2.194	2.040	529	60	195
Cu-232 rehydrated	75	2.196	2.047	432	22	440
	25	2.191	2.040	570	83	185

lw: linewidth

Table S3. EPR fitted parameters for the calcined and hydrate Cu-SAPO-34 and Cu-SAPO-18.

sample	species weight (%)	g_1	g_2	g_3	A_1 (MHz)	A_2 (MHz)	A_3 (MHz)	lw ₁ (MHz)	lw ₂ (MHz)	lw ₃ (MHz)	g	A (MHz)	lw (MHz)
Cu-SAPO-34	55	2.064	2.113	2.390	36	53	392	150	400	330			
calcined hydrate	45										2.170	95	925
Cu-SAPO-18	60	2.068	2.093	2.375	36	76	392	150	400	330			
calcined hydrate	40	2.191	2.040	570	83						2.165	95	950

lw: linewidth

Table S4. Atomic coordinates and thermal parameters for calcined and dehydrated Cu-SAPO-34.

Atom	<i>x</i>	<i>y</i>	<i>z</i>	Occupancy	<i>U</i> _{iso}	Multiplicity
Al1	0.2384(12)	0.2391(13)	0.0767(13)	1	0.0325(12)	9
Al2	0.7651(12)	0.7681(14)	0.8742(13)	1	0.0325(12)	9
P1	-0.0020(8)	0.2226(8)	0.0854(8)	1	0.0325(12)	9
P2	0.9915(8)	0.7673(8)	0.8699(8)	0.7	0.0325(12)	9
O1	0.9987(21)	0.2484(14)	0.9895(12)	1	0.0447(18)	9
O2	0.1175(10)	0.2441(16)	0.1089(16)	1	0.0447(18)	9
O3	0.2020(11)	0.1043(12)	0.1021(17)	1	0.0447(18)	9
O4	0.3098(11)	0.0167(11)	0.1533(14)	1	0.0447(18)	9
O5	0.9913(18)	0.7300(12)	0.9636(12)	1	0.0447(18)	9
O6	0.8788(11)	0.7545(15)	0.8408(17)	1	0.0447(18)	9
O7	0.8050(11)	0.9084(13)	0.8530(17)	1	0.0447(18)	9
O8	0.6897(11)	0.9984(11)	0.8027(13)	1	0.0447(18)	9
Si1	-0.0020(8)	0.2226(8)	0.0854(8)	0.3	0.0325(12)	9
Si2	0.9915(8)	0.7673(8)	0.8699(8)	0.3	0.0325(12)	9
Cu1	0.5414(21)	-0.0357(20)	0.0297(20)	0.155	0.0325(12)	9

Table S5. Selected bond lengths and angles for calcined and dehydrated Cu-SAPO-34.

Bond length / Å	Bond angle / °		
Al1-O	1.732(14)	O-Al1-O	109.4(10)
Al2-O	1.730(15)	O-Al2-O	109.4(10)
Al-O (Avg.)	1.731(15)	O-T-O (Avg.)	109.4(10)
P1(Si1)-O	1.531(15)	O-P1(Si1)-O	109.5(10)
P2(Si2)-O	1.541(15)	O-P2(Si2)-O	109.4(10)
P(Si)-O (Avg.)	1.536(15)	O-P(Si)-O (Avg.)	109.5(10)
T-O (Avg.)	1.633(15)	O-T-O (Avg.)	109.4(10)
Cu-O _{framework}	2.56(3)		

Table S6. Atomic coordinates and thermal parameters for calcined and dehydrated Cu-SAPO-18.

Atom	<i>x</i>	<i>y</i>	<i>z</i>	Occupancy	<i>U</i> _{iso}	Multiplicity
Al1	0.8930(6)	0.9612(6)	0.1670(5)	1	0.0075(6)	8
Al2	0.8830(6)	0.2227(6)	0.9409(5)	1	0.0075(6)	8
Al3	0.2278(6)	0.0967(7)	0.0491(6)	1	0.0075(6)	8
P1	0.7715(4)	0.0946(4)	0.0528(4)	0.75	0.0075(6)	8
P2	0.1099(4)	0.2289(4)	0.9351(4)	0.75	0.0075(6)	8
P3	0.1144(4)	0.9679(4)	0.1620(4)	0.75	0.0075(6)	8
O1	0.1806(9)	0.0499(10)	0.1306(6)	1	0.0190(13)	8
O2	0.1354(10)	0.1625(11)	0.0033(6)	1	0.0190(13)	8
O3	0.0041(5)	0.2566(6)	0.9458(5)	1	0.0190(13)	8
O4	0.8529(9)	0.1602(12)	0.0193(6)	1	0.0190(13)	8
O5	0.8121(9)	0.0439(10)	0.1218(6)	1	0.0190(13)	8
O6	0.0097(6)	1.0007(7)	0.1485(5)	1	0.0190(13)	8
O7	0.1372(9)	0.8613(8)	0.1317(6)	1	0.0190(13)	8
O8	0.3265(8)	0.1746(9)	0.0660(8)	1	0.0190(13)	8
O9	0.8671(7)	0.9621(7)	0.2568(4)	1	0.0190(13)	8
O10	0.8129(8)	0.3344(9)	0.9277(8)	1	0.0190(13)	8
O11	0.1250(9)	0.1636(8)	0.8679(6)	1	0.0190(13)	8
O12	0.2627(7)	-0.0104(11)	0.9977(9)	1	0.0190(13)	8
Si1	0.7715(4)	0.0946(4)	0.0528(4)	0.25	0.0075(6)	8
Si2	0.1099(4)	0.2289(4)	0.9351(4)	0.25	0.0075(6)	8
Si3	0.1144(4)	0.9679(4)	0.1620(4)	0.25	0.0075(6)	8
Cu1	0.003(5)	0.1275(12)	0.0616(11)	0.15	0.0075(6)	8

Table S7. Selected bond lengths and angles for calcined and dehydrated Cu-SAPO-18.

Bond length / Å		Bond angle / °	
Al1-O	1.730(9)	O-Al1-O	109.4(6)
Al2-O	1.732(9)	O-Al2-O	109.5(6)
Al3-O	1.739(9)	O-Al3-O	109.5(6)
Al-O (Avg.)	1.733(9)	O-T-O (Avg.)	109.5(6)
P1(Si1)-O	1.525(8)	O-P1(Si1)-O	109.5(6)
P2(Si2)-O	1.528(8)	O-P2(Si2)-O	109.4(6)
P3(Si3)-O	1.518(8)	O-P3(Si3)-O	109.5(6)
P(Si)-O (Avg.)	1.524(8)	O-P(Si)-O (Avg.)	109.4(6)
T-O (Avg.)	1.629(9)	O-T-O (Avg.)	109.5(6)
Cu-O _{framework}	2.24(5)		

Table S8. Crystallographic data for calcined and dehydrated Ni-SAPO-34 and Ni-SAPO-18.

	Ni-SAPO-34 ^a	Ni-SAPO-18 ^b
Chemical composition ^c	Ni _{2.6} H _{0.7} Al ₁₈ Si _{4.413,6} O ₇₂ 30.4H ₂ O	Ni _{2.5} Al ₂₄ Si ₅ P ₁₉ O ₉₆ 37.2H ₂ O
Data collection		
Wavelength / Å	1.54056	1.54056
Diffractometer	Debye-Scherrer	Debye-Scherrer
geometry		
Sample	rotating 0.5 mm capillary	rotating 0.5 mm capillary
Scanned region / 2θ°	3.0 – 70.0	5.0 – 70.0
Step size / 2θ°	0.1	0.1
Unit cell		
Chemical formula	Ni _{1.8} Al ₁₈ Si ₆ P ₁₂ O ₇₂	Ni _{1.4} Al ₂₄ Si _{4.8} P _{19.2} O ₉₆
Space group	R 3	C 1 2/c 1
a / Å	13.7089(2)	13.6760(3)
b / Å	13.7089(2)	12.8261(3)
c / Å	15.0663(3)	18.6162(4)
β / °		90.048(8)
Volume / Å ³	2452.10(9)	3265.46(7)
Rietveld refinement		
Refined region / 2θ°	5.0 – 70.0	6.0 – 70.0
% of SAPO-34		5.8
R _{wp}	0.056	0.036
R _p	0.042	0.028
R _F ²	0.072	0.037
X ²	3.47	1.64

(a) Ni-SAPO-34 was prepared in presence of Ni-DETA as SDA using the gel composition Al(OH)₃ : 0.61 H₃PO₄ : 0.25 SiO₂ : 40 H₂O : 0.15 Ni²⁺-DETA. (b) Ni-SAPO-18 was prepared in the presence of Ni-232 as SDA using the gel composition reported in the experimental section.

(c) Determined combining EDX, TGA and AAS.

Table S9. Atomic coordinates and thermal parameters for calcined and dehydrated Ni-SAPO-34.

Atom	<i>x</i>	<i>y</i>	<i>z</i>	Occupancy	<i>U</i> _{iso}	Multiplicity
Al1	0.2291(9)	0.2225(11)	0.0385(12)	1	0.0483(7)	9
Al2	0.7706(10)	0.7725(11)	0.8281(11)	1	0.0483(7)	9
P1	0.0032(8)	0.2324(8)	0.0336(8)	0.667	0.0483(7)	9
P2	0.9992(8)	0.7730(8)	0.8349(8)	0.667	0.0483(7)	9
O1	-0.0037(16)	0.2628(12)	-0.0606(10)	1	0.0560(14)	9
O2	0.1167(8)	0.2432(11)	0.0613(13)	1	0.0560(14)	9
O3	0.1836(9)	0.0793(10)	0.0519(14)	1	0.0560(14)	9
O4	0.3265(9)	0.0184(8)	0.0968(10)	1	0.0560(14)	9
O5	0.9912(15)	0.7306(11)	0.9290(11)	1	0.0560(14)	9
O6	0.8902(8)	0.7645(11)	0.7985(14)	1	0.0560(14)	9
O7	0.802(1)	0.909(1)	0.8214(14)	1	0.0560(14)	9
O8	0.6672(9)	0.9698(8)	0.7763(11)	1	0.0560(14)	9
Si1	0.0032(8)	0.2324(8)	0.0336(8)	0.333	0.0483(7)	9
Si2	0.9992(8)	0.7730(8)	0.8349(8)	0.333	0.0483(7)	9
Ni1	0.0004	0.0002	0.0769(15)	0.085	0.0483(7)	9
Ni2	0.4594(26)	0.4167(25)	0.0093(27)	0.108	0.0483(7)	9

Table S10. Selected bond lengths and angles for calcined and dehydrated Ni-SAPO-34.

Bond length / Å		Bond angle / °	
Al1-O	1.727(11)	O-Al1-O	109.5(8)
Al2-O	1.725(11)	O-Al2-O	109.5(8)
Al-O (Avg.)	1.726(11)	O-T-O (Avg.)	109.5(8)
P1(Si1)-O	1.537(11)	O-P1(Si1)-O	109.4(8)
P2(Si2)-O	1.533(11)	O-P2(Si2)-O	109.4(8)
P(Si)-O (Avg.)	1.535(11)	O-P(Si)-O (Avg.)	109.4(8)
T-O (Avg.)	1.630(11)	O-T-O (Avg.)	109.4(8)
Ni1-O _{framework}	2.219(12)		
Ni2-O _{framework}	2.16(4)		

Table S11. Atomic coordinates and thermal parameters for calcined and dehydrated Ni-SAPO-18.

Atom	<i>x</i>	<i>y</i>	<i>z</i>	Occupancy	<i>U</i> _{iso}	Multiplicity
Al1	0.8903(5)	0.9578(5)	0.1666(4)	1	0.0109(7)	8
Al2	0.8789(4)	0.2208(5)	0.9389(4)	1	0.0109(7)	8
Al3	0.2296(5)	0.0944(5)	0.0503(4)	1	0.0109(7)	8
P1	0.77300(29)	0.09608(29)	0.05433(29)	0.8	0.0109(7)	8
P2	0.10860(27)	0.23014(27)	0.93642(27)	0.8	0.0109(7)	8
P3	0.11799(28)	0.97148(28)	0.16559(28)	0.8	0.0109(7)	8
O1	0.1839(7)	0.0486(8)	0.1305(5)	1	0.0197(12)	8
O2	0.1378(8)	0.1658(9)	0.0045(5)	1	0.0197(12)	8
O3	0.0025(4)	0.2594(5)	0.9445(4)	1	0.0197(12)	8
O4	0.8498(7)	0.1608(10)	0.0170(5)	1	0.0197(12)	8
O5	0.8156(7)	0.0477(8)	0.1219(5)	1	0.0197(12)	8
O6	0.0114(4)	0.9956(5)	0.1515(4)	1	0.0197(12)	8
O7	0.1385(7)	0.8614(6)	0.1346(5)	1	0.0197(12)	8
O8	0.3297(6)	0.1719(6)	0.0661(6)	1	0.0197(12)	8
O9	0.8624(5)	0.9618(6)	0.25528(30)	1	0.0197(12)	8
O10	0.8105(6)	0.3332(7)	0.9242(6)	1	0.0197(12)	8
O11	0.1278(7)	0.1640(6)	0.8700(5)	1	0.0197(12)	8
O12	0.2639(5)	-0.0096(9)	0.9951(7)	1	0.0197(12)	8
Si1	0.77300(29)	0.09608(29)	0.05433(29)	0.2	0.0109(7)	8
Si2	0.10860(27)	0.23014(27)	0.93642(27)	0.2	0.0109(7)	8
Si3	0.11799(28)	0.97148(28)	0.16559(28)	0.2	0.0109(7)	8
Ni1	0.0100(31)	0.1208(10)	0.0608(8)	0.18	0.0109(7)	8

Table S12. Selected bond lengths and angles for calcined and dehydrated Ni-SAPO-18.

Bond length / Å		Bond angle / °	
Al1-O	1.729(7)	O-Al1-O	109.4(5)
Al2-O	1.735(7)	O-Al2-O	109.5(5)
Al3-O	1.739(7)	O-Al3-O	109.5(5)
Al-O (Avg.)	1.735(7)	O-T-O (Avg.)	109.5(5)
P1(Si1)-O	1.517(6)	O-P1(Si1)-O	109.5(5)
P2(Si2)-O	1.527(6)	O-P2(Si2)-O	109.5(5)
P3(Si3)-O	1.514(6)	O-P3(Si3)-O	109.4(5)
P(Si)-O (Avg.)	1.519(6)	O-P(Si)-O (Avg.)	109.4(5)
T-O (Avg.)	1.627(7)	O-T-O (Avg.)	109.5(5)
Ni-O _{framework}	2.28(3)		

Reference

- [S1] J. D. Hanawalt, H. W. Rinn, L. K. Frevel, *Anal. Chem.*, 10 (1938) 475-512.
- [S2] T. Sawada, K. Fukumaru, H. Sakurai, *Chem. Pharm. Bull.*, 44 (1996) 1009–1016.
- [S3] R. Garcia, I.J. Shannon, A.M.Z. Slawin, W. Zhou, P.A. Cox, P.A. Wright, *Microporous Mesoporous Mater.*, 58 (2003) 91–104.
- [S4] D.J. Szalda, E. Fujita, R. Sanzenbacher, H. Paulus, H. Elias, *Inorg. Chem.*, 33 (1994) 5855–5863.